Manufacturing Rev. **5**, 11 (2018)

https://doi.org/10.1051/mfreview/2018009

Manufacturing Review
Available online at:
https://mfr.edp-open.org

RESEARCH ARTICLE OPEN ACCESS

Effect of the thickness reduction of specimens on the limit strains in thermomechanical tensile tests for hot-stamping studies

Connor Lane, Zhutao Shao*, Kailun Zheng, and Jianguo Lin

Department of Mechanical Engineering, Imperial College London, London SW7 2AZ, UK

Received: 14 May 2018 / Accepted: 4 July 2018

Abstract. Sheet metal formability under hot stamping conditions has been evaluated using a novel planar testing system developed previously, being used within a Gleeble machine. Nevertheless, the specimen design with the central recess was not standardised, and the thickness reduction was not applied to the dog-bone type of specimen for testing at the uniaxial straining state. In this paper, effect of thickness reduction of dog-bone specimens on limit strain measurement under hot stamping conditions is investigated, and two types of dog-bone specimens without and with central recess are presented. Thermomechanical uniaxial tensile tests were performed at various deformation temperatures and strain rates, ranging from 370–510 °C and 0.01–1/s, respectively, by using the developed biaxial testing system in the Gleeble. The distributions of temperature and axial strain along gauge region of the two types of specimen were measured and compared. The specimen with consistent thickness had a better uniformity of temperature and strain distributions, compared to that with thickenss reduction. Forming limits for both types of specimen were also determined using the section-based international standard method. It is found that the accuracy of the calculation of forming limits based on the use of specimen with thickness reduction was highly dependent on the selection of the stage of the deformation of the specimen.

Keywords: Strain measurement / hot stamping / uniaxial tensile test / thermomechanical property / thickness reduction / AA6082

1 Introduction

The increasing demand for fuel-efficiency is a major challenge facing by the automotive industry in order to reduce energy consumption and air pollution [1]. The development of lightweighting strategies for vehicles' weight reduction is a feasible way to improve the energy efficiency and decrease CO_2 emissions. Lightweight materials, such as aluminium alloy, magnesium alloy and composites, are increasingly used to replace steels for manufacturing vehicles' body structures [2,3]. However, the applications of high-strength aluminium alloys are restricted by the poor formability at room temperature since panel components with complex geometries cannot be formed [4]. This makes the evaluation and the improvement of alloys formability become necessary. In addition, post heat treatment is usually required after forming to further increase component strength, which may result in low dimensional accuracy and increase manufacturing costs. To address these issues, advanced forming technologies, such as hydroforming, superplastic forming [5], quick plastic forming [6], and warm/hot stamping processes [7,8], have been developed. Forming aluminium alloy sheets at elevated temperatures enables to utilise significantly improved formability of the material and deform sheets into complex geometries [9]. Among the variety of high-temperature forming techniques, Hot Form and Quench (HFQ®) [10] is one of the leading techniques for the manufacture of high-strength complex-shaped aluminium alloy panel components [11,12]. In this process, the blank first experiences solution heat treatment (SHT) to dissolve precipitates and inclusions, resulting in a more ductile microstructure. The heat treated blank is then quickly transferred to a forming press to be hot stamped into particular shapes of die profiles. The deformed component is held firmly in the closed die for a specific time to quench and simultaneously freeze the sheet microstructure. For heat-treatable alloys, the part can then be artificially aged in order to obtain increased strength through the growth of dispersed precipitates [13].

A conventional and useful tool, forming limit diagram (FLD) represented by forming limit curves (FLCs), is commonly used to evaluate formability of sheet metals under different forming conditions. The FLC represents

* e-mail: z.shao12@imperial.ac.uk

Table 1. Chemical composition of AA6082.

Element	Si	Fe	Cu	Mn	Mg	Cr	Zn	Ti	Al
Weight proportion (%)	0.90	0.38	0.08	0.42	0.70	0.02	0.05	0.03	Balance

boundaries between uniform deformation and the beginning of necking which is likely to induce material failure or fracture [14]. Experimental methodologies, such as Nakajima and Marciniak methods, have been developed and used to determine FLCs at cold forming conditions, and they are the most commonly used methods. Banabic [14] summarised other theoretical and numerical methods for FLD prediction, such as the modified maximum force criterion (MMFC) proposed by Hora et al. [15]. But most of models need to be calibrated by experimental formability data. The use of cruciform specimen for experimental characterisation of formability is an alternative approach and has been applied for FLD determination at room temperature [16]. Main advantages have been found [17] by using cruciform specimens, including the ability to directly control the strain path, to apply complex linear and nonlinear loading paths, and to avoid the friction effect. In terms of cruciform specimen design, three features have been validated to be advantageous [16]: radii between adjacent arms reducing stress concentration in the corners; slits in the arms distributing the load more evenly to the gauge section and reducing load sharing in the arms; a thickness reduction leading to the high stress and strain in the gauge section and inducing deformation failure in the specimen central region [16].

Hot stamping and HFQ® processes have introduced complex deformation conditions, such as heating and cooling with controlled heating and cooling rates, to control the microstructural evolution. This makes the evaluation of formability become complicated since conventional methods of determining FLCs are normally applicable only for isothermal conditions. To address the limitations, a novel planar biaxial testing system, dedicated to testing under hot stamping conditions, has been established and developed by Shao et al. [18,19]. This test facility is the first testing system being capable of determining FLCs under hot stamping conditions. Three types of specimens were used for testing under different temperatures, strain rates and strain paths in a Gleeble which was applied to control accurately temperatures, heating and cooling rates during testing. The thickness of the central gauge region of the cruciform specimen is reduced by equally recessing from both sides, while the dog-bone specimen used has a constant thickness. The effect of the thickness reduction on the forming limit measurement has not been investigated.

Effect of sheet thickness on forming limits determined at room temperature has been studied by several researchers [20–23]. Dilmec et al. [22] conducted Nakajima experiments for rolled AA2024-T4 sheets with different thicknesses, and concluded that an increase in sheet thickness raised the level of FLCs. Hashemi et al. [23] reduced the thickness of a St14 steel sheet by grinding and evaluated sheet forming limits using Nakajima tests. The results showed that the effect of sheet thickness on the FLC was little, but the manufacturing process used to achieve thickness reduction might change the material formability unless it would not alter the material microstructure. These studies were performed at cold forming condition by specimens with overall different thicknesses. For the specimens used in the formability testing system proposed by Shao et al. [18] for hot stamping applications, the reduction of thickness was achieved by mechanical milling so that specimen microstructure remained during specimen machining. Also, SHT in the HFQ® process is able to resolve other possible differences of microstructure during thermomechanical testing. Since the temperature within the recess is controlled by resistance heating and air cooling in the Gleeble, a non-isothermal temperature distribution, due to the grip cooling effect, could potentially result in non-uniform deformation and measured inaccurate forming limits [24]. This may become worse by introducing a recess in the specimen.

The aim of this study was to develop a thorough understanding of the effect of a central recess on the uniformities of temperature and deformation, and on determined forming limits for aluminium alloy 6082 for hot stamping applications by using the developed biaxial testing system. This research was able to provide guides for standardising the design of specimens for this formability test and improve the accuracy of determined FLDs of alloys for hot stamping applications. To achieve this aim, a series of comparative thermomechanical tensile tests were performed by using specimens without and with thickness reduction. Effects on temperature distribution, strain uniformity and forming limit evaluations were analysed using a digital image correlation (DIC) system. The analysis reported in this paper also contributes to enhancement of understanding of alloy viscoplastic deformation characteristics under hot stamping conditions.

2 Experimental programme

2.1 Material and specimen design

The as-received material used in this study was heat treatable AA6082 with a thickness of 1.5 mm. The initial temper was T6 condition. The chemical composition is given in Table 1. Figure 1 shows the geometries and dimensions of specimens, namely (a) without thickness reduction and (b) with thickness reduction. The specimens were machinced along longitudinal sheet rolling direction. This design with constant thickness of 1.5 mm was used to evaluate forming limits at the uniaxial tensile state in [19] and it is named as the Type 1 specimen in the following discussion. Figure 1 (b) shows the dimensions of the specimen with a thickness reduction of 0.4 mm by milling away from both sides at the gauge zone and it is referred to

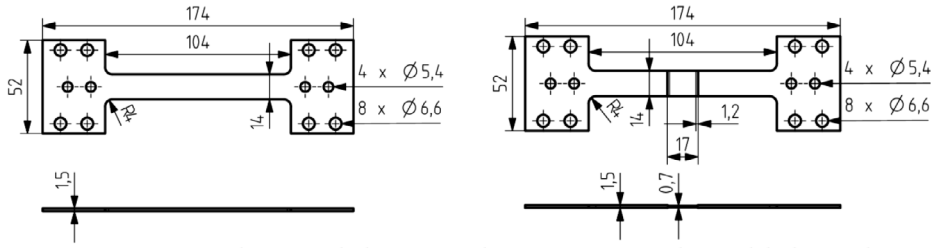

(a) Type 1 specimen with constant thickness *(b) Type 2 specimen with central thickness reduction*

Fig. 1. Dimensions of the dog-bone type of specimens without (a) and with (b) thickness reduction (dimensions in mm).

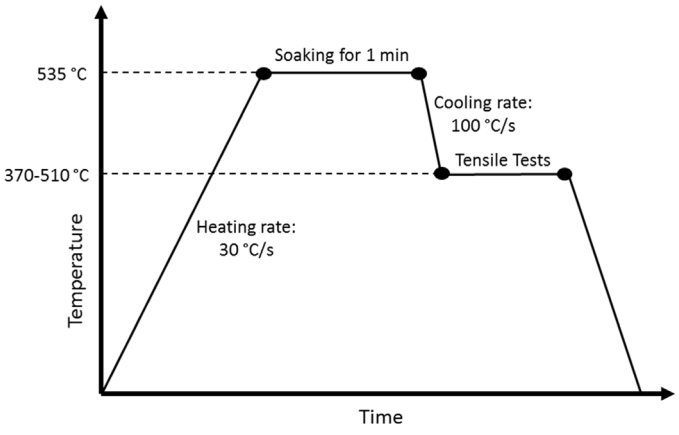

Fig. 2. A schematic showing the temperature profiles for evaluating the formability of AA6082 under HFQ® conditions.

as the Type 2 specimen. A length of 17 mm of the reduction region was designed to achevie the consistency with the cruciform specimens used in the previous work of [19].

2.2 Test procedure

Figure 2 shows the predefined temperature profile of AA6082 under HFQ® conditions [19]. The specimens were heated to 535 °C at a constant heating rate of 30 °C/s, soaked for 1 min and cooled to specified deformation temperatures at a cooling rate of 100 °C/s. Then, the specimen was uniaxially stretched at the temperature levels with different stretching rates. In this study, the tensile tests were performed at elevated temperatures of 370 °C, 440 °C and 510 °C. The temperatures were selected according to the forming conditions of a typical HFQ® process. Three different strain rates adopted were 0.01/s, 0.1/s, and 1/s since FLDs are strain rate dependent and linearity of strain rate before necking is required to determine forming limits. For the control of each strain rate, the constant value of strain rate was obtained before testing by programming the relationship between the Gleeble stroke and the processing time by taking into account the geometric relationship of the planar testing mechanism. The strain rate of each test will be calculated again after testing to be verified for each test. The matrix of test conditions is summarised in Table 2. Each test condition was repeated three times by using the developed biaxial testing system to ensure the repeatability.

Table 2. Test matrix of high-temperature uniaxial tensile tests.

T (°C)	Strain rate (/s)		
	0.01	0.1	1
510		x	
440	x	x	x
370		x	

2.3 Measurement methods

2.3.1 Temperature measurement

Thermocouples were welded on the mid-width line of both types of specimens to measure the temperature distribution in the specimens during testing. Thermocouple locations are shown in Figure 3. The selections are marked as T1 (the mid-length), T2 (5 mm from the mid-length), T3 (10 mm from the mid-length), T4 (For Type 1 is 15 mm from the mid-length, for Type 2 is 20 mm from the mid-length) and T5 (For Type 1 only is 30 mm from the mid-length). The temperature at the T1 position was monitored and controlled by using resistance heating and air cooling in the Gleeble. Measurements of the temperature distributions were conducted without stretching specimens. The axial temperature distribution at the elevated temperatures 370, 440, 510 and 535 °C was averaged and compared.

2.3.2 Axial strain measurement

Uniaxial tensile tests were conducted using the novel biaxial test system [18] based on the Gleeble 3800, as shown in Figure 4. A pattern of white dots on a black background was sprayed on the specimen surface to enable the strain measurement by the DIC system with a high-speed camera which was used to record the deformation history of the specimen. Different framing rates were used for each of the different experimental strain rates. Deformation at strain rates of 0.01/s, 0.1/s and 1/s were captured at respective framing rates of 25 fps, 50 fps and 500 fps with a resolution of 1280 × 1024 pixels. A detailed description of the test set-up can be found in [18,19]. Full-field strain and specimen failure were recorded during the entire deformation history to enable the detailed analysis of strain distribution.

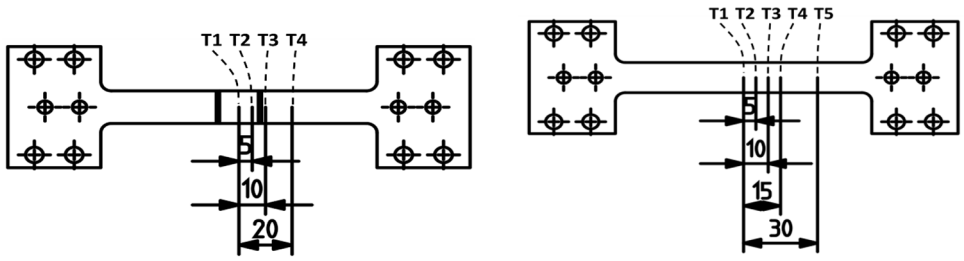

(a) Type 1 *(b) Type 2*

Fig. 3. Locations of the welded thermocouples.

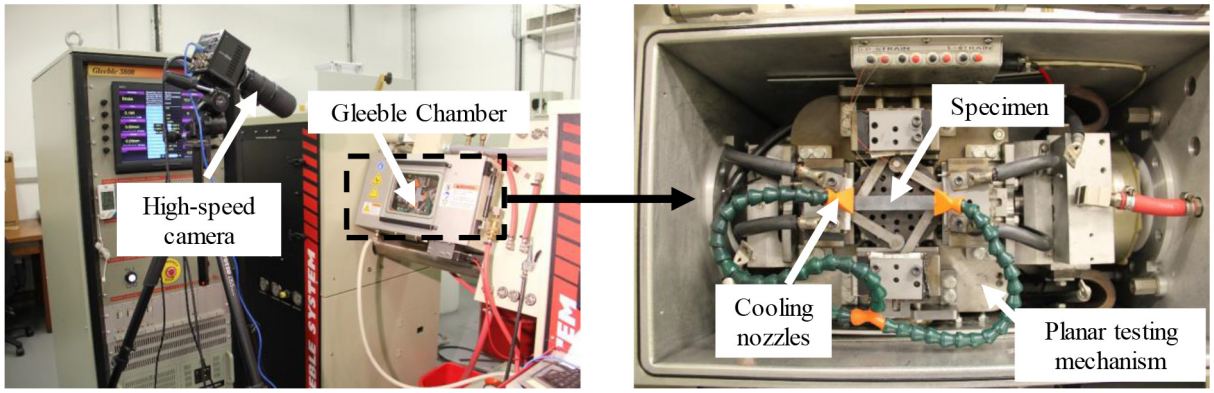

Fig. 4. The novel in-plane testing system with the set-up for thermo-mechanical tensile tests.

Table 3. Measured temperature differences for the specimen design of Type 1.

T_1 (0 mm)	ΔT_2 (5 mm)	ΔT_3 (10 mm)	ΔT_4 (15 mm)	ΔT_5 (30 mm)
535	−6	−10	−27	−120
510	−7	−10	−26	−109
440	−5	−9	−21	−89
370	−8	−9	−19	−75

Table 4. Measured temperature differences for the specimen design of Type 2.

$T1$ (0 mm)	ΔT_2 (5 mm)	ΔT_3 (10 mm)	ΔT_4 (20 mm)
535	−16	−63	−119
510	−15	−59	−108
440	−11	−45	−84
370	−9	−36	−67

2.3.3 Limit strain measurement

Forming limits at the uniaxial straining state were evaluated according to the section-based method described in the international standard ISO 12004-2 [25]. This method has already been implemented in the ARAMIS software. The basic principles are: three cross-sections are positioned perpendicular to the crack to obtain strain data along the gauge region, and then an inverse parabola is fitted on the bell-shaped curves for the determination of major and minor strains. The peak points of the fitted parabolas are used as the limit strains. This international standard has been commonly used for formability tests at isothermal conditions but no standard exists for the determination of limit strains under hot stamping conditions.

3 Results and discussion

3.1 Temperature distribution

Tables 3 and 4 show the measured temperature differences between the defined locations and the reference point T_1, i.e. $\Delta T_i = T_i - T_1$, i.e. ($i = 2$–5). Figure 5 shows the fitted experimental results of temperature drops (circular symbols with solid lines for Type 1 specimens and square symbols with dash lines for Type 2 specimens).

The temperature drops can be observed from the mid-length to the clamping regions of both types of specimens. The temperature differences, for Type 1 and Type 2 specimens at 10 mm, were 10 °C and 63 °C, respectively. With the decrease of maximum temperature, the temperature drop reduced for both types of specimens. Between T1

Table 5. Total deformation time under various testing conditions.

Strain rate (/s)/ Temperature (°C)	0.01/440	0.1/440	0.1/370	0.1/510	1/440
Type 1	37.2s	7.2s	7.1s	7.4s	0.9s
Type 2	14.1s	3.5s	3.2s	3.2s	0.4s

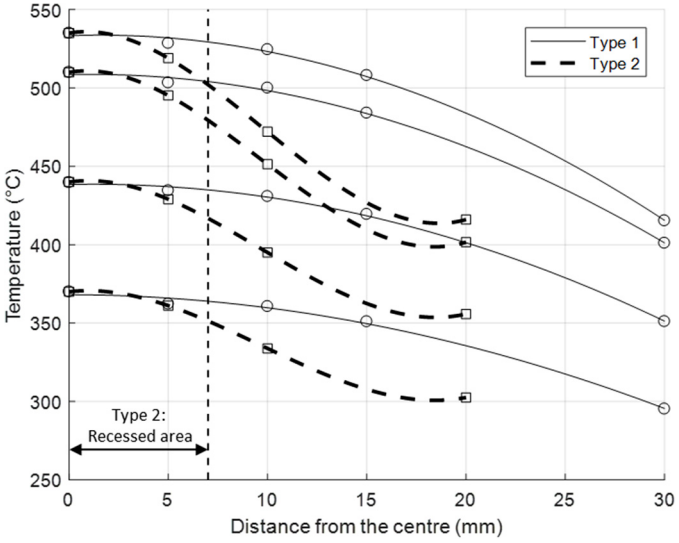

Fig. 5. Comparison of the temperature distribution for the two types of specimen design.

and T3 for Type 1 specimen, it was 10 °C (1.9%) from the reference temperature of 535 °C, and 9 °C (2.4%) from the reference temperature of 370 °C, respectively. Type 2 specimens showed a difference between T1 and T3 of 63 °C (12%) for the reference temperature of 535 °C and 36 °C (10%) from the reference temperature of 370 °C, which was more distinct compared to those of Type 1. The mismatch between both types of specimens is due to the thickness difference and the nature of resistance heating adopted in the Gleeble. The input current supplied by the Gleeble was controlled by the closed loop feedback control system based on the output temperature of reference point T1. According to Joule's law, the power of heating P is proportional to the resistance R and the square of the current I. Although the current flow is consistent within the specimen, the electrical resistance R changes as the specimen thickness changes. The resistance of specimen is determined by the cross-section area of A, the electrical resistivity of ρ, and the specimen length of l. The higher resistance of the thinned middle zone for Type 2 specimens led to heating differences and hence larger temperature drops towards the clamping regions, compared with Type 1 specimens without thickness reduction. The Gleeble grip cooling effect is considered to be more significant for Type 2 specimens, since the required total heating power to heat up specimens to the same temperature level is lower for Type 2 specimens compared to that for Type 1 specimens.

3.2 Axial strain measurement

Thermomechanical tensile tests were conducted for the testing conditions as shown in Table 2. The beginning of deformation is marked with $t=0$ and the moment of fracture is marked as the fracture time $t=t_f$. The total deformation time is summarised in Table 5. Tests conducted using Type 2 specimens showed about half of the total deformation time compared to those using Type 1 specimens at the same corresponding testing conditions. The shorter time to fracture was caused by the thickness reduction in Type 2 specimens, since the recessed area induced a stress concentration within the specimen. As the grips stretched the specimen with thickness reduction at the designated strain rates, the elongation was localised in the recess region whereas the outer region was strained less, which led to high deformation strain level and high strain rate. Therefore, it can be seen that the Type 2 specimen tended to failure earlier than the Type 1 specimen. In order to unify the time scale of relative deformation stage between these two types of specimen and better compare the strain evolution for both types, a dimensionless normalised deformation time t/t_f is introduced, where the normalized deformation time equals to 0 which represents the beginning of deformation for both types of specimen, and the value equals to 1 representing the moment of fracture. The strain evolution in the gauge region at different deformation stages within the range of 20–100% normalised time are shown in Figure 6. The distance from the center refers to the original unstretched position. These positions were tracked during deformation and localised strains were plotted accordingly.

As can be seen in Figure 6, strain distribution for Type 1 specimens were uniformly distributed before a normalised deformation time of 35%, but for Type 2 specimens, strains tended to be non-uniformly distributed along the gauge region from the beginning of deformation, although the maximum strains achieved in each deformation stage were similar for both types of specimens. It was also found that the non-uniformity of strain distribution increased with the increase of deformation temperature. This is mainly due to the fact that the absolute temperature drop from the mid-length to the clamping regions was larger at high temperatures, especially for the Type 2 specimen. Similar trends can be observed for testing at other different strain rates. Therefore, a new gauge length, instead of using parallel gauge length, needs to be defined in order to obtain localised strain data for the determination of forming limit strains. Within this new gauge length, named as effective gauge length in this paper, the deformation is considered to be uniform before the onset of necking. A smaller effective gauge length should be used for the Type 2 specimen due to

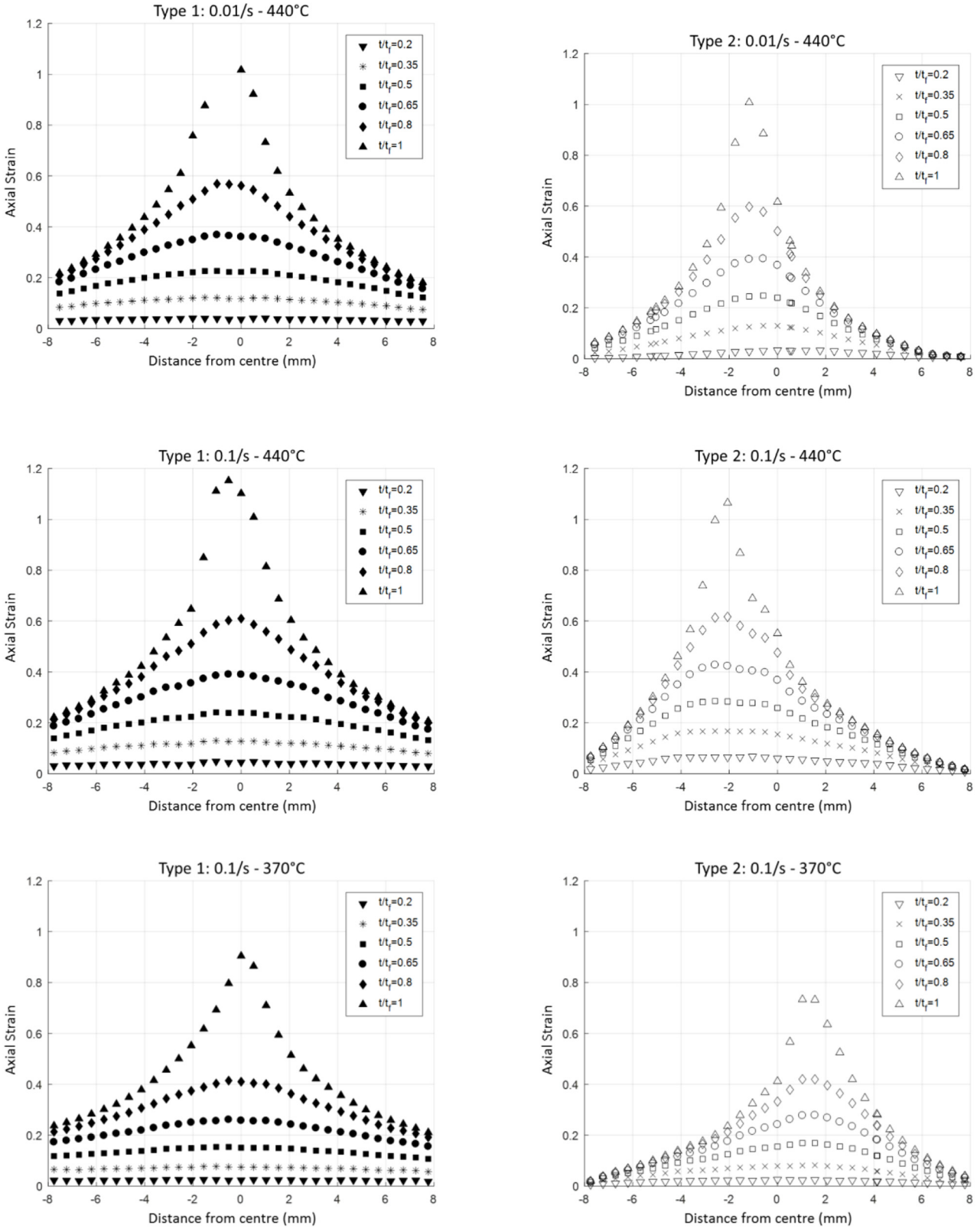

Fig. 6. Comparison of local axial strain distribution at different deformation stage (specimen type, testing condition aremarked on top of each figure).

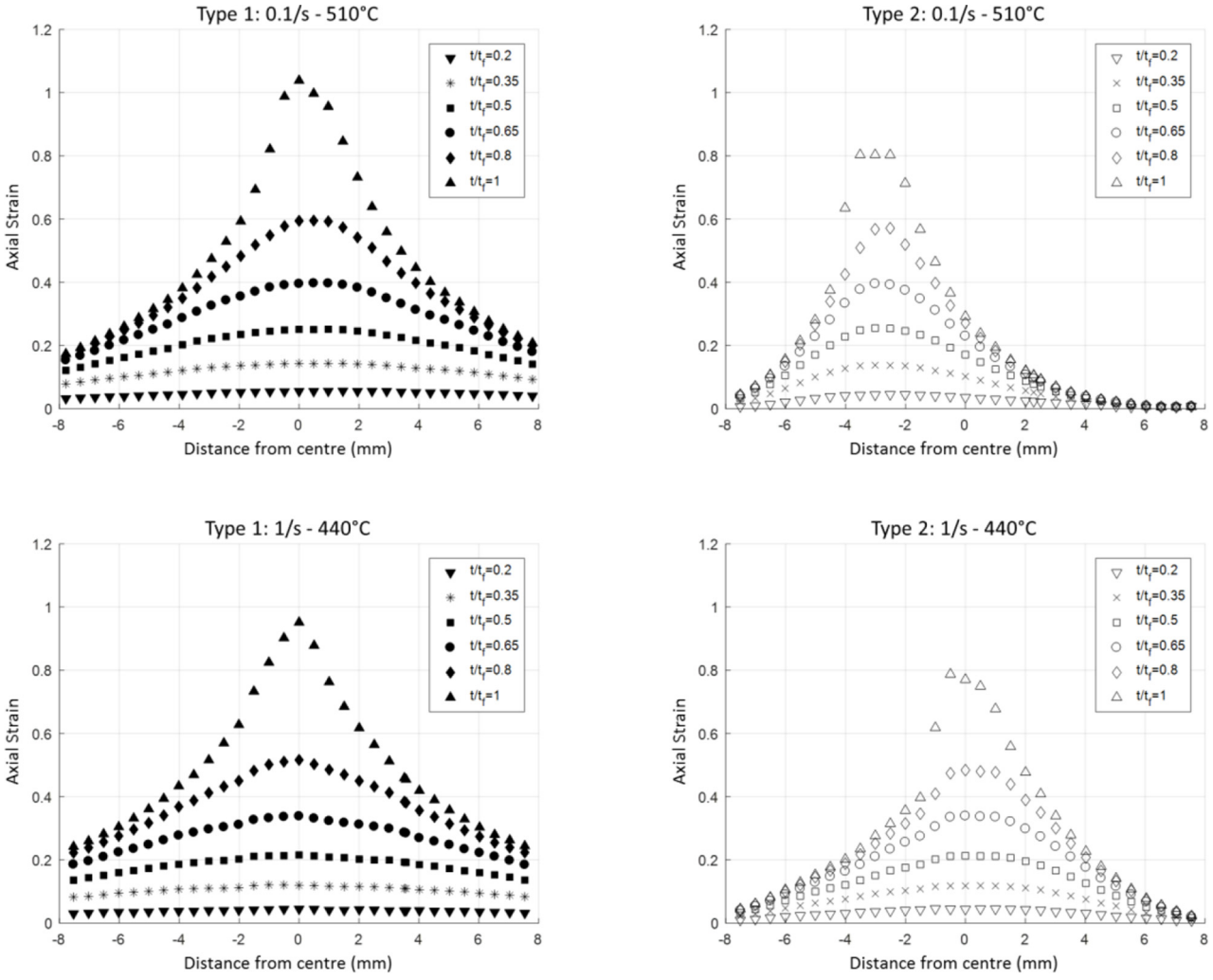

Fig. 6. (*Continued*).

the inhomogeneity of strain distribution. However, the defined gauge length cannot be too small which would lead to measured results being highly sensitive to the localised strain, and probably not sufficient strain data can be collected along the defined gauge length for limit strain determination according to the standardised section-based methods.

Figure 7 compares the average strain through entire deformation history based on the definition of gauge lengths of 6 mm and 10 mm for Type 2 and Type 1 of specimen, respectively, deformed at the test condition of 440 °C and 0.1/s. It can be seen that the total strain to failure for the Type 2 specimen was 20–30% lower compared to that for the Type 1 specimen, and the average strain rate for the Type 2 specimen was 60–70% higher based on the new definition of gauge length. This can also been observed for testing under other conditions. Throughout the deformation, the strain rate increased gradually once the localised necking occurred. It is noted that the calculated average strain rate is dependent on the definition of effective gauge length, which can be determined by the analysis of the deformation history.

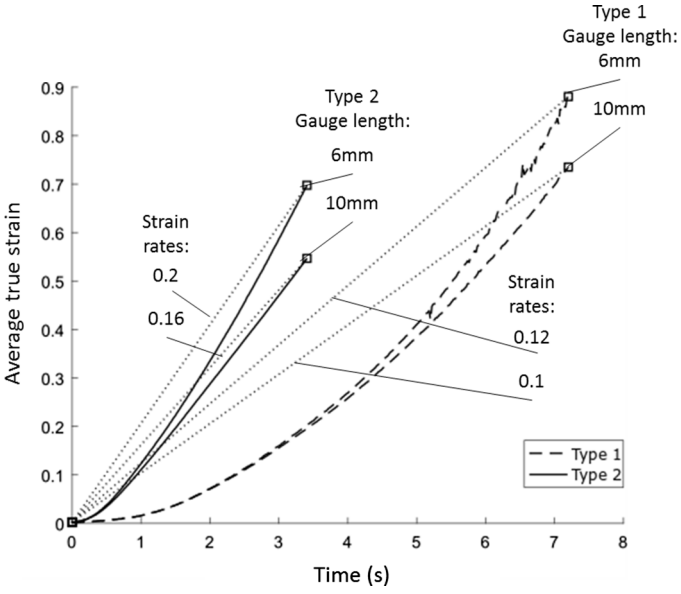

Fig. 7. Comparison of average strain rate for different definition of gauge at the deformation temperature of 440 °C and the strain rate of 0.1/s.

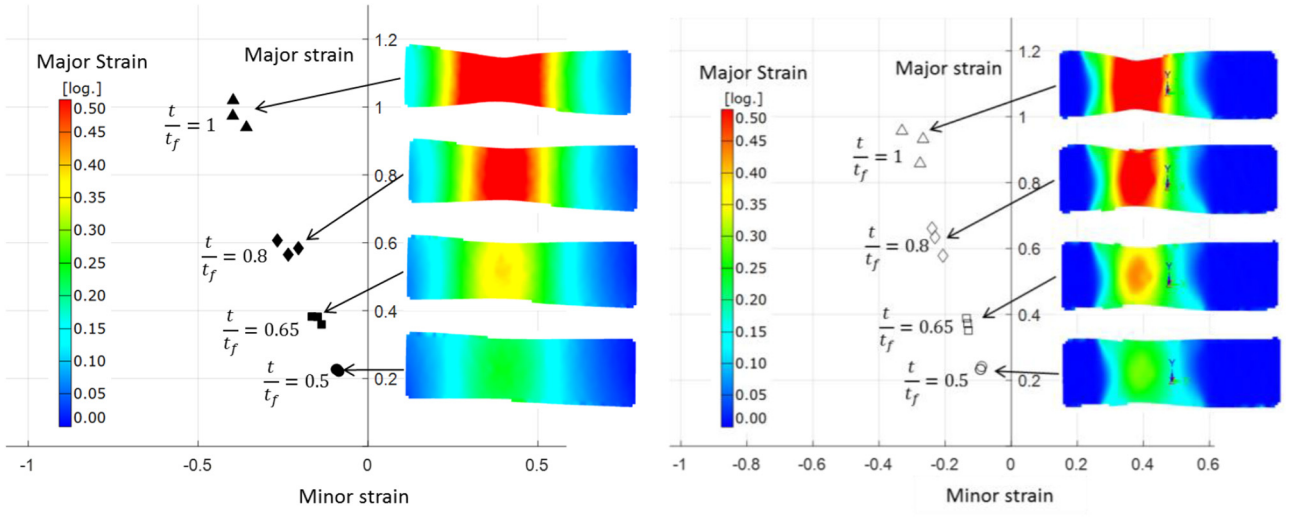

Fig. 8. Determined forming limit strains for different deformation stages at the temperature of 440 °C and strain rate of 0.1/s.

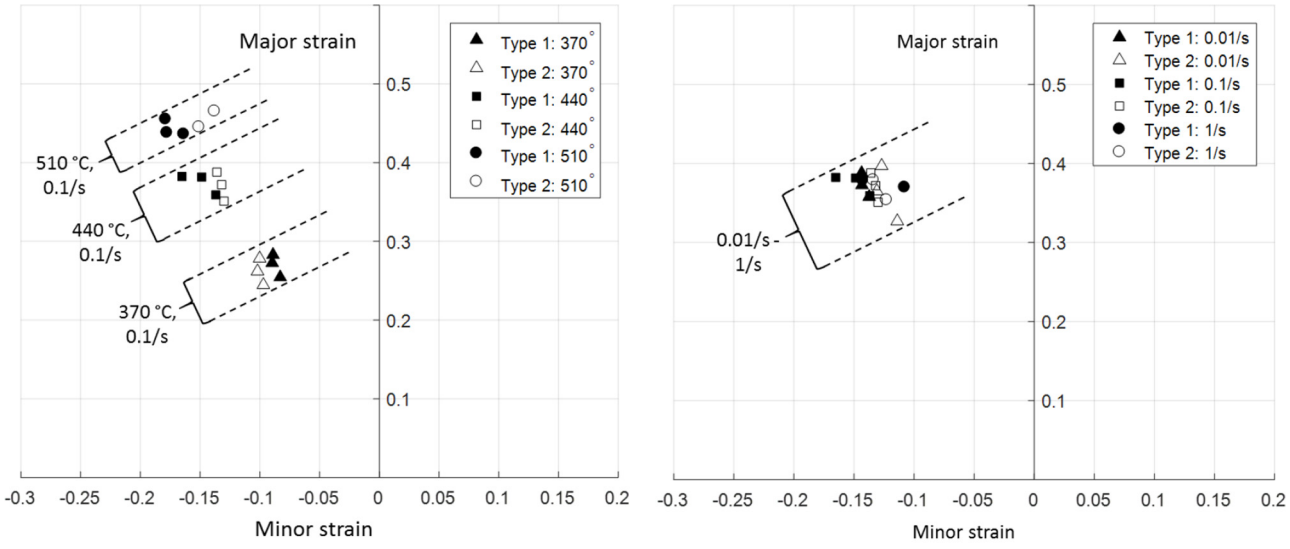

Fig. 9. Temperature and forming speed effects on the determined forming limits at a normalised deformation time of 65%.

3.3 Forming limit at uniaxial straining state

Following the international standard ISO 12004-2 [25], limit strains should be calculated by using the image of the last stage picture before the crack recorded by the DIC, corresponding to a normalised deformation time of 100%, since the deformation cannot be recorded by using conventional testing methods, which might cause concervative results of calculated forming limits. Since all specimens had already shown distinct necking by a normalised time of 65% according to images recorded by the high-speed camera, this stage was selected for Type 1 specimens to determine limit strains previously. It is noticed that the temperature gradient, especially for the Type 2 specimen, led to non-uniform deformation, which made the use of section-based method become difficult. The determined results of limit strains were dependent on the selection of the deformation stage. The limit strains determined using the section-dependent method based on different stages of images are shown in Figure 8, deformed at 440 °C and strain rate of 0.1/s. In Figure 8(a), for the Type 1 specimen, necking has occurred before the normalised time of 80% total deformation time. For the Type 2 specimen in Figure 8(b), the deformation was restricted in the recessed region from the beginning. For both types of specimen, it might not be appliacable to

explicitly identify the onset of necking by the section-based fitting method so that the determination of forming limits under hot stamping conditions is less accurate. Future work is suggested to identify a modified suitable time-dependent method to determine forming limits under hot stamping and HFQ® conditions.

Figure 9 shows limit strains determined for specimens without and with thickness reduction at different test conditions. The forming limits were determined at the normalised deformation time of 65%, which was selected as an example. Strain ratios of minor strain to major strain were typically between −0.35 and −0.4, which are within similar range for uniaxial tensile tests conducted in [19]. The determined limits of the Type 1 and Type 2 specimens at the selected normalised deformation time are very similar to each other and vary within a small error range, although the total deformation time was different. It is found that the forming limits increase with the increase of deformation temperature but they are not highly sensitive to strain rate at the uniaxial straining state. Similar trends were observed from previous study in [19].

4 Conclusions

In the study reported in this paper, the effect of thickness reduction on the strain limits of AA6082 obtained by thermomechanical tensile tests was investigated using a novel planar testing facility for formability evaluation under hot stamping conditions, based on which the following conclusions can be drawn:

- The non-uniformity of temperature distribution between the recess region and other consistent-thickness region in the specimens is increased due to the thickness variation, which lowers the uniformity of deformation and strain in the specimen. The specimen with consistent thickness has a higher uniformity of temperature and strain distribution compared to that with thickenss reduction.
- Tensile tests by using specimens with thickness reduction tend to have higher strain rate and lower total deformation time, but this effect can be reduced after normalising the deformation history to determine limit strains by following the section-based method.
- The resistance heating method is sensitive to the specimen dimensions. Increasing the length of recess region can potentially reduce the non-uniformity of temperature and strain distribution, which would lower the accuracy of measured limit strains.
- Applying the standardised section-based method for the determination of forming limits causes a higher error for testing by using specimen with thickness reduction under hot stamping conditions because the calculation of forming limits is dependent on the selection of the deformation stage. A suitable time-dependent method used for forming limit determination under hot stamping conditions needs to be developed in the future work.

Financial support from EPSRC Impact Acceleration Account Funding (grant number: EP/R511547/1) is gratefully acknowledged by the authors. Specimen machining by Advanced Manufacturing (Sheffield) Ltd. is gratefully acknowledged. HFQ® is a registered trademark of Impression Technologies Ltd. Impression Technologies Ltd. is the sole licensee for the commercialisation of the HFQ® technology from Imperial College London.

References

1. W.S. Miller, L. Zhuang, J. Bottema, A.J. Wittebrood, P.D. Smet, A. Haszler, A. Vieregge, Recent development in aluminium alloys for the automotive industry, Mater. Sci. Eng. A **280** (2000) 37–49
2. I. Polmear, Light alloys: from traditional alloys to nano-crystals, Butterworth-Heinemann, 2005, Oxford, United Kingdom
3. M.F. Ashby, D. Cebon, Materials selection in mechanical design, Le Journal de Physique IV, vol. 3, pp. C7–1, 1993
4. G.S. Cole, A.M. Sherman, Light weight materials for automotive applications, Mater. Charact. **35** (1995) 3–9
5. L. Lihui, L. Kangning, G. Cai, X. Yang, C. Guo, G. Bu, A critical review on special forming processes and associated research for lightweight components based on sheet and tube materials, Manuf. Rev. **1** (2014) 9
6. P.E. Krajewski, J.G. Schroth, Overview of quick plastic forming technology, in Materials science forum, 2007
7. N. Li, M.S. Mohamed, J. Cai, J. Lin, D. Balint, T.A. Dean, Experimental and numerical studies on the formability of materials in hot stamping and cold die quenching processes, in AIP Conference Proceedings, 2011.
8. P.A. Tebbe, G.T. Kridli, Warm forming of aluminium alloys: an overview and future directions, Int. J. Mater. Prod. Technol. **21** (2004) 24–40
9. P.J. Bolt, N.A.P.M. Lamboo, P.J.C.M. Rozier, Feasibility of warm drawing of aluminium products, J. Mater. Process. Technol. **115** (2001) 18–121
10. A. Foster, T.A. Dean, J. Lin, Process for forming aluminium alloy sheet components, Google Patents, 2012
11. R.P. Garrett, J. Lin, T.A. Dean, An investigation of the effects of solution heat treatment on mechanical properties for AA 6xxx alloys: experimentation and modelling, Int. J. Plast. **21** (2005) 1640–1657
12. H. Gao, Hot stamping of an Al–Li alloy: a feasibility study, Manuf. Rev. **3** (2016) 9
13. R.P. Garrett, J. Lin, T.A. Dean, Solution heat treatment and cold die quenching in forming AA 6xxx sheet components: feasibility study, Adv. Mater. Res. **6–8** (2005) 673–680
14. D. Banabic, Sheet metal forming processes: constitutive modelling and numerical simulation, Springer, 2010, Cluj Napoca, Romania
15. P. Hora, L. Tong, B. Berisha, Modified maximum force criterion, a model for the theoretical prediction of forming limit curves, Int. J. Mater. Form. **6** (2013) 267–279
16. A. Hannon, P. Tiernan, A review of planar biaxial tensile test systems for sheet metal, J. Mater. Process. Technol. **198** (2008) 1–13
17. I. Zidane, D. Guines, L. Leotoing, E. Ragneau, Development of an in-plane biaxial test for forming limit curve (FLC) characterization of metallic sheets, Meas. Sci. Technol. **21** (2010) 055701
18. Z. Shao, N. Li, J. Lin, T.A. Dean, Development of a new biaxial testing system for generating forming limit diagrams for sheet metals under hot stamping conditions, Exp. Mech. **56** (2016) 1489–1500

19. Z. Shao, N. Li, J. Lin, T. Dean, Formability evaluation for sheet metals under hot stamping conditions by a novel biaxial testing system and a new materials model, Int. J. Mech. Sci. **120** (2017) 149–158
20. A.A. Zadpoor, J. Sinke, R. Benedictus, The effects of thickness on the formability of 2000 and 7000 series high strength aluminum alloys, Key Eng. Mater. **410** (2009) 459–466
21. M. Dilmec, H.S. Halkaci, F. Ozturk, H. Livatyali, O. Yigit, Effects of sheet thickness and anisotropy on forming limit curves of AA2024-T4, Int. J. Adv. Manuf. Technol. **67** (2013) 2689–2700
22. R. Hashemi, A. Ghazanfari, K. Abrinia, A. Assempour, Forming limit diagrams of ground St14 steel sheets with different thicknesses, SAE Int. J. Mater. Manuf. **5** (2012) 60–64
23. Z. Shao, N. Li, J. Lin, T.A. Dean, Strain measurement and error analysis in thermo-mechanical tensile tests of sheet metals for hot stamping applications, Proc. Inst. Mech. Eng. Part C: J. Mech. Eng. Sci. **232** (2017) 1994–2008
24. I.S.O. Standard, 1200 4-2, Metallic materials-sheet and strip-determination of forming-limit curves-part, vol. 2, 2008
25. GOM mbH, ARAMIS, ARGUS, SVIEW User Manual – FLC Computation v6.1.1 and higher, 2009

Cite this article as: Connor Lane, Zhutao Shao, Kailun Zheng, Jianguo Lin, Effect of the thickness reduction of specimens on the limit strains in thermomechanical tensile tests for hot-stamping studies, Manufacturing Rev. **5**, 11 (2018)